

Critical dynamics govern the evolution of political regimes

Joshua Uhlig,^{1,*} Paula Pirker-Díaz,¹ Matthew Wilson,² Ralf Metzler,^{1,†} and Karoline Wiesner^{1,‡}

¹University of Potsdam, Institute for Physics & Astronomy, 14476 Potsdam, Germany

²University of South Carolina, Department of Political Science, Columbia, SC, USA

(Dated: March 9, 2026)

The emergence and decline of democratic systems worldwide raises fundamental questions about the dynamics of political change. Contrary to the idea of a stable endpoint of liberal democracy, recent backsliding towards less democratic regimes highlights the non-stationary nature of regime evolution. Here, we analyse the historical trajectories of countries within a two-dimensional regime space derived from the principal components of the Varieties of Democracy dataset. We observe weakly non-ergodic dynamics unfolding in an effective landscape characterised by sparse and shifting basins of stability. Step sizes and sojourn times characterising this dynamics follow heavy-tailed distributions near the critical regime, in which mean values appear to diverge. These facts point to the intermittent and heterogeneous nature of the regime change dynamics. A continuous time random walk model reproduces the dynamics of the three most recent decades with remarkable accuracy. Together, these results suggest that some aspects of political regime evolution follow universal stochastic principles, while remaining punctuated by unique historical pathways.

I. INTRODUCTION

Political systems evolve over time, but the dynamic nature of this change remains poorly understood. Classical theories of modernisation and democratic consolidation describe regime evolution as a gradual progression towards stable governance [1–3]. However, recent episodes of democratic backsliding and regime reversal challenge this idea [4]. Researchers also argue that political development is path-dependent, with each country following trajectories shaped by key moments in its history [5, 6]. It is not known whether political regimes evolve along unique historical paths or whether their trajectories are constrained by general dynamical laws.

To explore these dynamics, we draw on a subset of the Varieties of Democracy (V-Dem) dataset [7], which provides yearly measures of political characteristics for countries from 1900 to 2021. We represent each country’s position in a two-dimensional regime space defined by the first two principal components (PC1 and PC2), following Ref. [8]. PC1 corresponds to a democracy-autocracy axis, while PC2 reflects a trade-off between electoral capabilities and civil liberties [8]. The resulting two-dimensional PC1-PC2 plane is treated as a political regime space. Figure 1 shows all country-year points in this regime space, along with several well-known examples to provide intuition for its structure.

As countries evolve, they move through this space along trajectories. This suggests viewing regime evolution as a dynamical process unfolding over time. Approaches from sociophysics have increasingly applied concepts from statistical physics to collective social phenomena [9–11]. Stochastic models developed in statistical

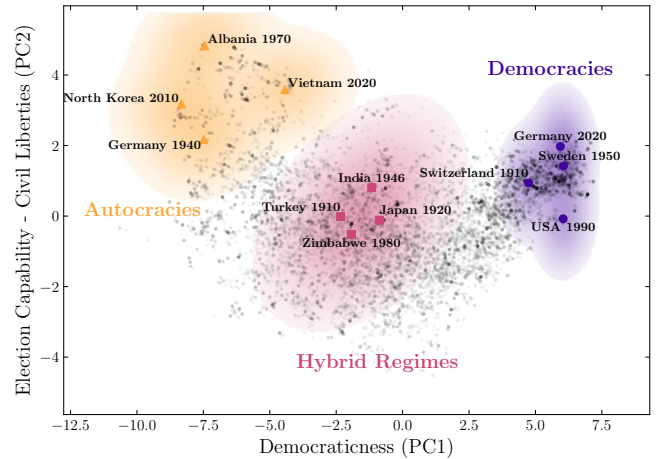


FIG. 1. All country-year observations in the PC1-PC2 political regime space. Selected examples indicate regions typically associated with democratic, autocratic, and hybrid regimes. These labels are illustrative and do not imply discrete regime classifications.

physics provide a natural framework for analysing such dynamics [12, 13]. Although originally developed to explain the motion of particles in fluids [14, 15], these models have since been applied to animal movement [16, 17], financial time series [18, 19], and human mobility [20]. Dedicated approaches to parameter regression, classification of the stochastic processes underlying the observation, as well as methods to identify change-points in the dynamics have been developed recently [21–24]. In parallel, diffusion-based analyses have been applied to political regime trajectories, uncovering dynamical structure in regime stability [25].

In our analysis, we find that regime trajectories exhibit near scale-free step size and sojourn time distributions and display weak ergodicity breaking. These features indicate that political regimes evolve through inter-

* joshua.uhlig@uni-potsdam.de

† rmetzler@uni-potsdam.de

‡ karoline.wiesner@uni-potsdam.de

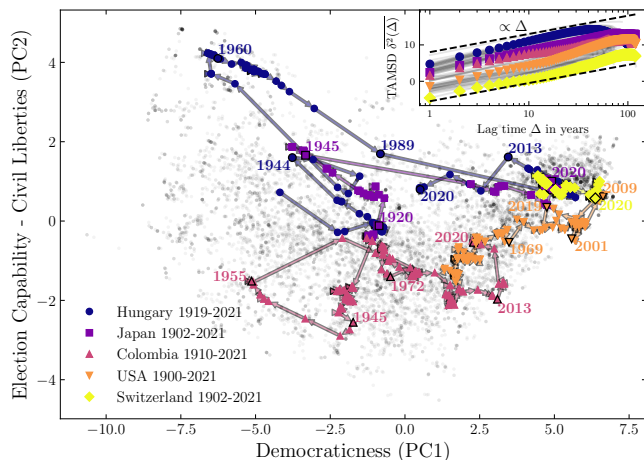


FIG. 2. **Representative regime trajectories in the two-dimensional political regime space.** Coloured symbols show selected country trajectories over time, superimposed on all country-year observations (black transparent dots). Inset: time-averaged mean-squared displacement (TAMSD) for the same countries.

mittent, path-dependent dynamics. We show that these patterns can be captured by a continuous time random walk (CTRW) [26] parameterised from the empirical distributions. The model reproduces both the average behaviour and the trajectory-level variability. Our findings show that political regime change appears to be simultaneously historically specific and dynamically universal.

II. RESULTS

A. Empirical regime dynamics

We analyse country trajectories in the two-dimensional regime space defined by the first two principal components of the V-Dem dataset: PC1 (democraticness) and PC2 (trade-off between electoral capability and civil liberties). Examples of some of the longest trajectories are shown in Fig. 2. They illustrate a broad spectrum of dynamical behaviours, ranging from gradual shifts to abrupt transitions. Most trajectories include periods with little or no change, sojourn times, interspersed with sudden shifts whose magnitude and direction vary from year to year.

Countries such as Hungary have explored large portions of the political space over the past century, while Japan and Colombia remained confined to a few regime regions separated by large jumps. Early in the 20th century, Japan was a monarchy and occupied the hybrid regime region, then shifted towards autocracy during the 1940s and, after World War II, moved rapidly into the democratic basin, where it has remained with only minor fluctuations. The United States shows a more gradual evolution towards the high-density democratic cluster,

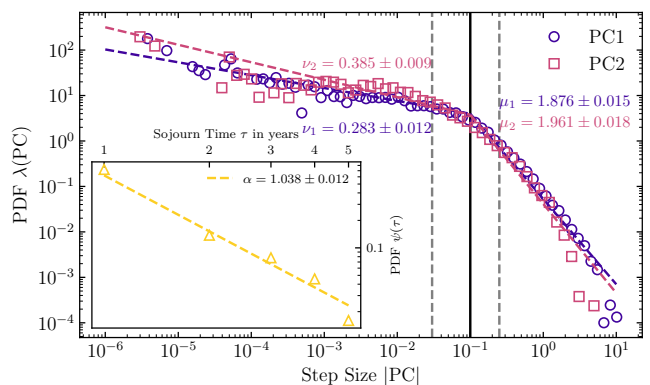


FIG. 3. **Step size and sojourn time PDFs in regime space.** Histograms show the PDFs of annual step sizes in PC1 and PC2; inset shows the normalised sojourn time PDF. Dashed coloured lines indicate maximum-likelihood power-law fits using a representative crossover point $PC_c = 0.1$ (black vertical line), with estimated exponents reported in the panels. Grey dashed lines indicate the range of crossover points considered.

with a reversal in recent years. Switzerland, by contrast, begins and remains within the democratic basin throughout its entire history.

The diversity of these trajectories becomes clearer when quantifying how much area of the regime space is explored over a time interval Δ . The time-averaged mean-squared displacement (TAMSD; inset of Fig. 2) reveals that individual country TAMSDs vary over nearly two orders of magnitude. The wide spread of individual TAMSD curves indicates weak ergodicity breaking [27–31], a hallmark of intermittent dynamics. In practical terms, this means that countries do not “sample” the political landscape uniformly: some remain trapped in stable configurations for decades, while others undergo rapid and repeated transitions. As a result, long-term behaviour remains strongly country-specific rather than averaging out across time. Formally, in such systems, time averages along single trajectories do not converge to the same value as averages taken across countries [27–31]. Countries undergoing major shifts, such as Hungary, display large displacements, whereas stable democracies, such as Switzerland, show minimal displacement. At small lag times, individual TAMSDs scale close to linearly with Δ , though some appear slightly super- or sub-linear. At large Δ , fewer points contribute to the average, producing irregular curves where country-specific trends dominate. For example, Japan’s TAMSD plateaus during its recent stability, while Hungary’s decreases during democratic backsliding.

A “step” refers to the change in a country’s position from one year to the next in the PC1-PC2 space, and the step size distribution characterises how large these changes typically are. Figure 3 shows the probability density functions (PDFs) $\lambda_i(PC_i)$ ($i = 1, 2$) of step sizes on log-log axes. Both dimensions exhibit two

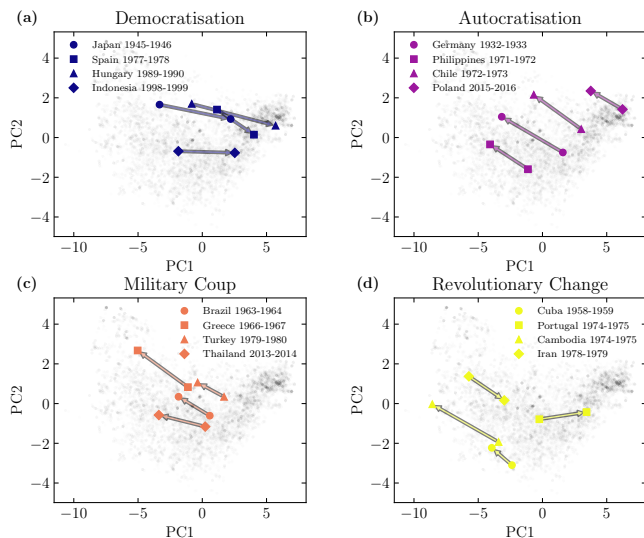


FIG. 4. **Representative examples of large regime transitions in the PC1-PC2 political regime space.** Arrows indicate one-year displacements associated with well-documented episodes of democratisation (a), autocratisation (b), military coups (c), and revolutionary change (d). These examples show that large movements in regime space correspond to substantive institutional ruptures, providing qualitative grounding for the heavy-tailed step-size statistics analysed in the main text.

distinct scaling regimes separated by a crossover scale. Small steps are common and approximately uniformly distributed, reflecting routine policy adjustments and incremental institutional change. In contrast, large steps follow a heavy-tailed PDF, corresponding to rare, abrupt regime shifts such as revolutions, coups, or breakdowns of political order. Figure 4 presents representative examples of large one-year displacements associated with well-documented institutional ruptures, including democratisation, autocratisation, coups, and revolutions. The crossover between these regimes is sharper in PC1, while PC2 shows a smoother change in slope, possibly reflecting a more continuous trade-off between civil liberties and electoral capability.

We model the step size PDFs as bimodal power-laws with a crossover point PC_c following

$$\lambda_i(PC_i) \propto \begin{cases} |PC_i|^{-\nu_i}, & PC_l \leq |PC_i| < PC_c, \\ |PC_i|^{-\mu_i}, & |PC_i| \geq PC_c, \end{cases} \quad (1)$$

where PC_l is the lower bound of the power-law (see Methods IV B). To characterise the tail behaviour, we estimate the exponents μ_i for a range of crossover points $PC_c \in [0.03, 0.25]$ (grey dashed lines in Fig. 3). Across this full range, the maximum-likelihood estimates remain within $\mu \approx 1.6..2.4$, i.e., near the critical regime $\mu = 2$ where the mean step size diverges (Appendix A). This shows that the heavy-tailed structure is robust and not an artefact of threshold choice. For clarity in presenta-

tion, we therefore report exponent values using a representative cutoff $PC_c = 0.1$. Together, these two scaling regimes indicate that frequent small adjustments and rare large transformations characterise how political systems change.

We next examine how long countries tend to remain in a given configuration before such changes occur.

The sojourn time PDF $\psi(\tau)$ (inset of Fig. 3) also appears to follow a power-law,

$$\psi(\tau) = \alpha \tau_0^\alpha \tau^{-(1+\alpha)}, \quad (2)$$

with a lower cutoff $\tau_0 = 1$ year, due to the temporal resolution. Here, sojourn times correspond to periods during which a country remains in approximately the same institutional configuration. A heavy-tailed PDF, therefore, implies that while many regimes change quickly, others persist for unusually long periods, yielding extended stability punctuated by rare, abrupt shifts. The discrete maximum-likelihood estimator (Eq. 5)) yields the exponent $\alpha \approx 1$. Thus, sojourn times are likewise near a critical threshold where mean values diverge, allowing both short and long intervals of political stasis. Together, these results reveal that countries exhibit near-critical, weakly non-ergodic regime dynamics, characterised by heavy-tailed step sizes and sojourn times.

B. Temporal stability of the regime space

Having characterised how countries move through the regime space, we now address a natural question: are there regions in this political landscape where regimes persistently stabilise, or is stability itself historically contingent? To identify regions of local stability, we compute first-passage times (FPTs) [32, 33], defined as the time a trajectory remains within a neighbourhood before exiting (see Methods IV C). This measure captures how long political systems persist near a given institutional configuration before undergoing substantial change. Spatially averaging FPTs by starting position reveals heterogeneous stability basins that shift over time (Fig. 5).

In the early period (1900-1930), two main zones of extended stability are visible. One lies around $PC_1 \approx 0$, encompassing colonies such as South Africa and monarchies like Hungary or Japan. The other corresponds to the democratic basin at high PC1 and low PC2 values.

Between 1930 and 1960, the hybrid regime region becomes increasingly isolated, with its surrounding area showing markedly reduced stability. This transition coincides with the erosion of imperial and monarchical systems worldwide. At the same time, the democratic area retains reduced but still moderately high FPTs, while the autocratic extreme begins to exhibit slightly longer FPTs, suggesting the emergence of a new stable configuration at this pole of the regime space.

From 1960 to 1990, the centres of stability shift decisively towards these extremes. Both the high PC1 democratic region and the low PC1 autocratic region display

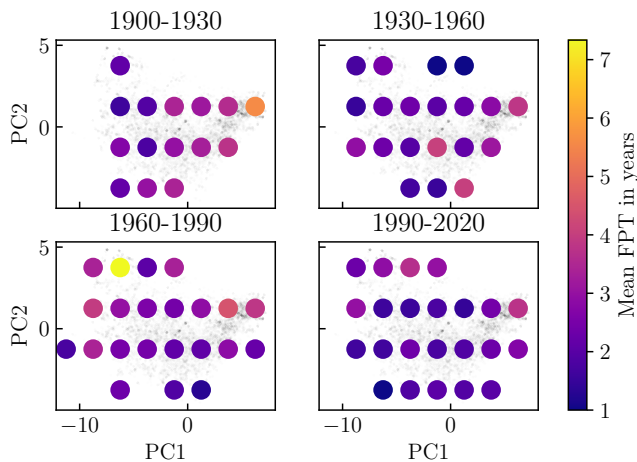


FIG. 5. Mean first-passage times (FPTs) in the regime space for successive 30-year windows. Warm colours indicate longer FPTs and thus greater local political stability, corresponding to prolonged residence near a given institutional configuration.

elevated FPTs. In the case of the autocratic region, up to twice the values seen in earlier decades appear. Deeply autocratic regimes such as Albania’s remain virtually static during this period, contributing to the extended persistence observed in that region.

In the most recent period (1990-2020), the democratic and autocratic poles remain the most stable regions, with reduced but similarly long FPTs in both areas. The FPT in the surrounding areas decays slowly to very short times ≈ 1 year, indicating broader but shallower stability zones.

Across the full time span, the democratic basin persists as the only consistent stable region. The early hybrid regime zone dissolves mid-century, giving way to an autocratic basin that weakens towards the present. Overall, these results reveal a rugged, shifting landscape of political stability, in which enduring regime configurations are rare and increasingly polarised between democratic and autocratic extremes. Next, we test whether the dynamics can arise from a minimal stochastic mechanism.

C. Modelling regime dynamics

The combination of heavy-tailed step sizes, scale-free sojourn times, and weak ergodicity breaking is characteristic of systems well described by a CTRW, making it a natural minimal model for regime dynamics. In a CTRW, a walker makes jumps separated by random sojourn times [26, 30], which here correspond to regime shifts and periods of institutional inertia. We simulate a two-dimensional CTRW parameterised by the empirically estimated step size and sojourn time PDFs.

We compare the simulated trajectories to empirical regime paths from 1990-2020, where uninterrupted data

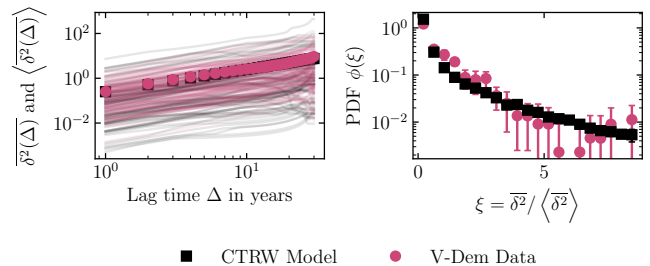


FIG. 6. Time-averaged mean-squared displacement (TAMSD) for empirical trajectories and continuous time random walk (CTRW) simulations. Lines show individual TAMSDs, symbols indicate their ensemble averages, and the corresponding amplitude scatter PDF $\phi(\xi)$ is shown alongside.

are available for $N = 108$ countries. As shown in Fig. 6, the ensemble-averaged TAMSD $\langle \delta^2 \rangle$ from the CTRW closely matches the empirical behaviour. Moreover, the amplitude scatter of individual TAMSDs, quantified by the PDF $\phi(\xi)$ [29, 34], is reproduced as well, capturing the characteristic spread associated with weak ergodicity breaking. Similar levels of agreement hold across the full robust range of PC_c values (Appendix A). Thus, the model captures both the mean dynamical behaviour and the trajectory-to-trajectory variability. The overall agreement is striking for such a simple model.

These results demonstrate that near-critical CTRW dynamics are sufficient to reproduce the essential statistical structure of regime evolution, including intermittent movement, heterogeneous stability, and persistent non-ergodicity.

III. DISCUSSION

Political regime evolution is often framed either as universal development [1–3] or as the result of historical events and path dependence [5, 6]. Our findings show that both views are correct, but incomplete: regime trajectories are historically specific, yet they also follow shared dynamical patterns. Countries move through political regime space in a manner characterised by intermittent dynamics, combining periods of stability with occasional large-scale transitions. The PDFs of both step sizes and sojourn times follow heavy-tailed, near scale-free forms, and the TAMSD exhibits strong trajectory-to-trajectory variability. Together, these signatures indicate weak ergodicity breaking, in which long-term political trajectories do not converge towards a shared path but remain strongly shaped by historical contingencies and institutional legacies [27–31].

The stability landscape inferred from first-passage times shows that persistent regime configurations are sparse and historically shifting. A basin associated with hybrid systems is evident in the early 20th century but

dissolves mid-century. A stability region appears at the autocratic extreme during the mid-century period, before weakening in recent decades. In contrast, the democratic basin is the only stability region that persists across the entire time span. These patterns indicate a rugged and evolving landscape of viability, in which the stability of political configurations depends on the broader historical context.

When stable states are sparse, movement patterns with tail exponents near $\mu \approx 2$ maximise the likelihood of reaching them [35–40]. The same exponents and the resulting interplay between long residence times and occasional large transitions arise in heterogeneous environments in which walkers must balance the risks and rewards of exploration [41]. The empirical step size and sojourn time PDFs fall in this range, indicating that countries move as if navigating a heterogeneous landscape of viable configurations. Concurrently, power-law distributions of sojourn times are characteristic of diffusion and transport dynamics in living biological cells [42, 43] as well as in human travel [20]. The implication is not that countries choose such movement strategies, but that they arise from the structure of the stability landscape.

A CTRW parameterised by empirically measured sojourn time and step size PDFs reproduces both the average regime movement and the degree of weak ergodicity breaking. This suggests that the interplay between long residence times and rare, large transitions is sufficient to generate the observed patterns. Political systems, therefore, appear to operate near a critical boundary between rigidity and volatility: stable enough to preserve institutions in the absence of shocks, yet sufficiently flexible to undergo abrupt reconfiguration when internal or external pressures accumulate.

The model abstracts away from the causes of specific transitions, such as economic crises, social movements, leadership turnovers or international alignment. The examples shown in Fig. 4 correspond to well-documented episodes of democratisation, autocratisation, military coups, and revolutionary change, including Japan’s post-war transition, Spain and Hungary’s democratic openings, Germany’s 1933 authoritarian consolidation, Chile’s 1973 coup, and the Iranian and Cuban revolutions. Although historically distinct, these events contribute to the same heavy-tailed distribution of step sizes, indicating that diverse political ruptures share common stochastic dynamics. Future work could integrate external influences like geopolitical shocks, economic crises or collective movements by including additional stochastic or deterministic forces that act on the countries. However, verifying such extensions is challenging given the annual resolution and fragmented nature of the empirical trajectories.

Taken together, these results show that political regime change is shaped both by country-specific histories and by general dynamical patterns. While the events driving transitions may differ across cases, the way regimes move through the political space follows a shared struc-

ture. These movements reflect the shape of the regime landscape and the limited number of stable configurations within it.

IV. METHODS

A. Data preprocessing

To ensure continuity when computing time-averaged observables, we restrict analysis to trajectory segments containing at least ten consecutive years without missing entries. For the comparison between empirical data and model simulations, we use the period 1990-2020, during which 108 uninterrupted country trajectories are available.

B. Exponent estimation

For visualisation, we plot histograms of the step size PDFs in Fig. 3, where bins are chosen on a log scale using the outlier resilient Freedman Diaconis estimator [44]. To estimate the exponents ν_i and μ_i of the PDFs $\lambda_i(\text{PC}i)$ (Eq. (1)) we use maximum likelihood estimation (MLE). The lower bound of the PDF $\text{PC}_l = 10^{-6}$, required for exponent estimation, is chosen as the order of magnitude of the smallest observed step size. For the tail exponent μ_i the exponent by MLE is given by [45]

$$\mu_i = 1 + n \left[\sum_{j=1}^n \ln \left(\frac{|\text{PC}i|_j}{\text{PC}_c} \right) \right]^{-1}. \quad (3)$$

For the bounded first regime we determine ν_i numerically by maximising the log-likelihood [46]

$$-\nu \sum_{j=1}^m \ln |\text{PC}i|_j + m \ln \left(\frac{1 - \nu}{(\text{PC}_c)^{1-\nu} - (\text{PC}_l)^{1-\nu}} \right). \quad (4)$$

For the discrete sojourn times, no binning is needed, and the normalised counts are displayed in the inset of Fig. 3. We use the corresponding discrete MLE estimator [45]

$$\alpha = N \left[\sum_{i=1}^N \ln \left(\frac{\tau_i}{\tau_0 - 1/2} \right) \right]^{-1}. \quad (5)$$

C. First passage time

To quantify local stability in the regime space, we compute the FPT for each trajectory. For a given starting point, the FPT is defined as the first time step at which the trajectory exits a circle of radius 0.1 in the PC1-PC2 plane. This radius corresponds to the approximate crossover scale between small and large regime changes

(see Fig. 3 and Appendix A). If a trajectory does not cross the threshold within the observable period, the FPT is treated as undefined and excluded from averaging. FPTs are computed for every possible starting year along each trajectory and then spatially binned across the PC1-PC2 plane using square bins of side length 2.5. This bin size ensures that each bin contains data from multiple countries while avoiding unnecessary coarse-graining. The mean FPT per bin defines the stability landscape shown in Fig. 5.

D. Weak ergodicity breaking

The TAMSD of a trajectory $x(t)$ of length T is defined as [34]

$$\overline{\delta^2(\Delta, T)} = \frac{1}{T - \Delta} \int_0^{T-\Delta} [x(t + \Delta) - x(t)]^2 dt, \quad (6)$$

where Δ is the lag time. The TAMSD quantifies how much the trajectory spreads on average over the regime space over a given time interval. We use the TAMSD instead of the ensemble-averaged MSD because country trajectories have different lengths and starting conditions, making the construction of an ensemble difficult.

For ergodic processes such as Brownian motion [14, 15, 34], the time and ensemble averages coincide in the long-time limit, and individual TAMSD curves collapse onto the ensemble mean. In contrast, many complex systems exhibit a broad spread of TAMSD values across trajectories. The averaged TAMSD,

$$\langle \overline{\delta^2(\Delta)} \rangle = \frac{1}{N} \sum_{i=1}^N \overline{\delta^2(\Delta)}_i, \quad (7)$$

is then not representative of any individual realisation. This phenomenon is known as weak ergodicity breaking [27–31].

A CTRW naturally produces weak ergodicity breaking when either the mean sojourn time [28, 29, 31] or the second moment of the step size PDF diverges [47, 48]. In such cases, the corresponding diffusion equation becomes fractional in both space and time. In particular, when the mean sojourn time diverges, the process exhibits memory, meaning the probability of being at a particular position depends on the full history of the trajectory, rather than only its current state.

E. CTRW simulations

The V-Dem indices are bounded by construction [7], and therefore their principal components are also bounded. To ensure that simulated trajectories remain realistic, we impose an upper cutoff on the step size PDFs. We choose these upper bounds as the largest observed empirical step sizes in each dimension ($PC1_{\max} \approx$

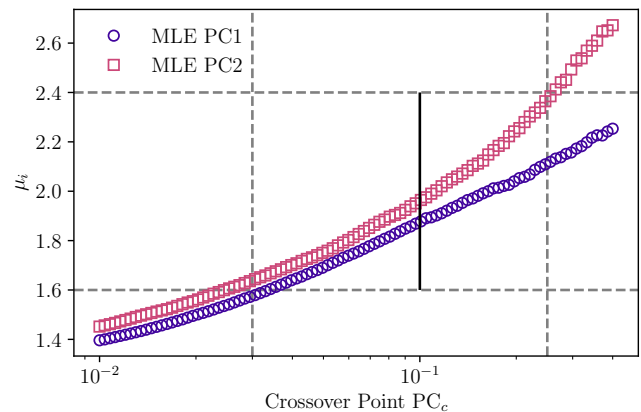


FIG. A.1. Maximum-likelihood estimates of the tail exponents μ_i of the step size PDFs $\lambda_i(PC_i)$ ($i = 1, 2$) for different crossover points PC_c . The vertical grey lines indicate the range of reasonable crossover points $PC_c \in [0.03, 0.25]$, and the black line marks the representative value $PC_c = 0.1$ used in the main text.

11.16 and $PC2_{\max} \approx 5.53$), which prevents unrealistically large jumps while avoiding additional parameterisation of the spatial bounds.

The CTRW is simulated as follows. At each update, a sojourn time τ is drawn from the empirical sojourn time PDF $\psi(\tau)$ and rounded to the nearest integer (reflecting the yearly temporal resolution). After the sojourn period, step sizes in PC1 and PC2 are independently sampled from their respective heavy-tailed PDFs, subject to the upper bounds above. This process is repeated until the desired total trajectory length is reached.

To compare to the empirical period 1990–2020, we simulate an ensemble of 10^4 trajectories, each with a duration of $T = 31$ years.

Appendix A: Robustness of the crossover point

The exponent of the power-law tail depends on the choice of the crossover point PC_c , so we assess the influence of this choice here. Figure A.1 shows the estimated tail exponents over a wide range of PC_c values. Within the empirically reasonable range $PC_c \in [0.03, 0.25]$, the tail exponents remain within $\mu_i \approx 1.6..2.4$, i.e., close to the critical regime $\mu = 2$. The absence of a plateau is consistent with the bounded nature of the V-Dem data, suggesting a PDF with a cutoff, potentially exponential in nature.

To evaluate the effect of this variation on the dynamics, we simulate the CTRW using the exponent values corresponding to the lower bound, upper bound, and representative crossover point $PC_c = 0.1$. Figure A.2 shows that both the ensemble-averaged TAMSD $\langle \overline{\delta^2(\Delta)} \rangle$ and the amplitude scatter PDF $\phi(\xi)$ remain in close agreement with the empirical data in all cases.

Thus, the heavy-tailed structure of regime shifts and

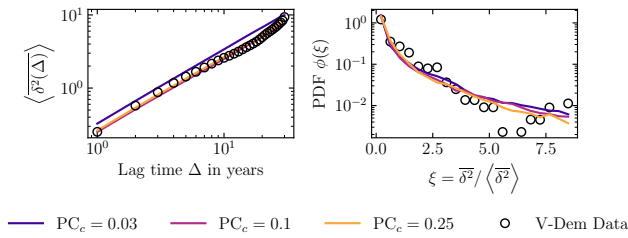


FIG. A.2. Ensemble-averaged TAMSD $\langle \delta^2(\Delta) \rangle$ and TAMSD amplitude scatter PDFs $\phi(\xi)$ for CTRW simulations with different crossover points, compared to empirical data (1990-2020).

the resulting CTRW dynamics are robust to the choice of PC_c , and do not depend on fine-tuning of this param-

eter. This confirms that the key results reflect structural features of the empirical PDFs rather than the specific choice of crossover threshold.

DATA AVAILABILITY

The V-Dem Dataset is publicly available at <https://v-dem.net/data/>, and the data subset used in this work can be found at <https://github.com/JoshuaUhlig/RegimeDynamics>.

CODE AVAILABILITY

All code used in this study is available at <https://github.com/JoshuaUhlig/RegimeDynamics>.

- [1] S. M. Lipset, Some social requisites of democracy: Economic development and political legitimacy, *Am. Political Sci. Rev.* **53**, 69–105 (1959).
- [2] D. C. North, *Structure and change in economic history* (W.W. Norton, 1981).
- [3] F. Fukuyama, The end of history?, *Natl. Interest* **16**, 3 (1989).
- [4] E. Grillo, Z. Luo, M. Nalepa, and C. Prato, Theories of democratic backsliding, *Ann. Rev. Political Sci.* **27**, 381 (2024).
- [5] P. Pierson, Increasing returns, path dependence, and the study of politics, *Am. Political Sci. Rev.* **94**, 251–267 (2000).
- [6] J. Mahoney, Path dependence in historical sociology, *Theory Soc.* **29**, 507 (2000).
- [7] M. Coppedge et al., V-dem codebook v12, Varieties of Democracy (V-Dem) Project (2022).
- [8] K. Wiesner, S. Bien, and M. C. Wilson, The principal components of electoral regimes: Separating autocracies from pseudo-democracies, *R. Soc. Open Sci.* **11**, 240262 (2024).
- [9] C. Castellano, S. Fortunato, and V. Loreto, Statistical physics of social dynamics, *Rev. Mod. Phys.* **81**, 591 (2009).
- [10] S. Galam, *Sociophysics* (Springer, 2012).
- [11] E. Ubaldi, R. Burioni, V. Loreto, and F. Tria, Emergence and evolution of social networks through exploration of the adjacent possible space, *Commun Phys* **4**, 28 (2021).
- [12] R. Klages, G. Radons, and I. M. Sokolov, *Anomalous transport: Foundations and applications* (Wiley-VCH, 2008).
- [13] P. L. Krapivsky, S. Redner, and E. Ben-Naim, *A Kinetic View of Statistical Physics* (Cambridge University Press, 2010).
- [14] A. Einstein, Über die von der molekularkinetischen Theorie der Wärme geforderte Bewegung von in ruhenden Flüssigkeiten suspendierten Teilchen, *Ann. Phys.* **322**, 549 (1905).
- [15] P. Langevin, Sur la théorie du mouvement brownien, *C. R. Acad. Sci. Paris* **146**, 530 (1908).
- [16] O. Vilck, Y. Orchan, M. Charter, N. Ganot, S. Toledo, R. Nathan, and M. Assaf, Ergodicity breaking in area-restricted search of avian predators, *Phys. Rev. X* **12**, 031005 (2022).
- [17] P. G. Meyer, A. G. Cherstvy, H. Seckler, R. Hering, N. Blaum, F. Jeltsch, and R. Metzler, Directedness, correlations, and daily cycles in springbok motion: From data via stochastic models to movement prediction, *Phys. Rev. Res.* **5**, 043129 (2023).
- [18] A. G. Cherstvy, D. Vinod, E. Aghion, A. V. Chechkin, and R. Metzler, Time averaging, ageing and delay analysis of financial time series, *New J. Phys.* **19**, 063045 (2017).
- [19] S. Ritschel, A. G. Cherstvy, and R. Metzler, Universality of delay-time averages for financial time series: Analytical results, computer simulations, and analysis of historical stock-market prices, *J. Phys. Complex.* **2**, 045003 (2021).
- [20] D. Brockmann, L. Hufnagel, and T. Geisel, The scaling laws of human travel, *Nature* **439**, 462–465 (2006).
- [21] G. Muñoz-Gil, H. Bachimanchi, J. Pineda, B. Midtvedt, G. Fernández-Fernández, B. Requena, Y. Ahsini, S. Asghar, J. Bae, F. J. Barrantes, and et al., Quantitative evaluation of methods to analyze motion changes in single-particle experiments, *Nat. Comm.* **16**, 6281 (2025).
- [22] H. Seckler and R. Metzler, Bayesian deep learning for error estimation in the analysis of anomalous diffusion, *Nat. Comm.* **13**, 6717 (2022).
- [23] G. Muñoz-Gil, G. Volpe, M. A. Garcia-March, E. Aghion, A. Argun, C. B. Hong, T. Bland, S. Bo, J. A. Conejero, N. Firbas, and et al., Objective comparison of methods to decode anomalous diffusion, *Nat. Comm.* **12**, 6253 (2021).
- [24] X. Feng, H. Sha, Y. Zhang, Y. Su, S. Liu, Y. Jiang, S. Hou, S. Han, and X. Ji, Reliable deep learning in anomalous diffusion against out-of-distribution dynamics, *Nat. Comput. Sci.* **4**, 761–772 (2024).
- [25] P. Pirker-Diaz, M. C. Wilson, S. Beier, and K. Wiesner, Scaling laws of political regime dynamics: Stability of democracies and autocracies in the twentieth century, *R. Soc. Open Sci.* **12**, 250457 (2025).

- [26] E. W. Montroll and G. H. Weiss, Random Walks on Lattices. II, *J. Math. Phys.* **6**, 167 (1965).
- [27] J. P. Bouchaud, Weak ergodicity breaking and aging in disordered systems, *J. Phys. I* **2**, 1705 (1992).
- [28] G. Bel and E. Barkai, Weak ergodicity breaking in the continuous-time random walk, *Phys. Rev. Lett.* **94**, 240602 (2005).
- [29] Y. He, S. Burov, R. Metzler, and E. Barkai, Random time-scale invariant diffusion and transport coefficients, *Phys. Rev. Lett.* **101**, 058101 (2008).
- [30] R. Metzler and J. Klafter, The random walk's guide to anomalous diffusion: A fractional dynamics approach, *Phys. Rep.* **339**, 1 (2000).
- [31] J. H. P. Schulz, E. Barkai, and R. Metzler, Aging renewal theory and application to random walks, *Phys. Rev. X* **4**, 011028 (2014).
- [32] S. Redner, *A Guide to First-Passage Processes* (Cambridge University Press, 2001).
- [33] R. Metzler, G. Oshanin, and S. Redner, *First-Passage Phenomena and Their Applications* (World Scientific, 2014).
- [34] R. Metzler, J.-H. Jeon, A. G. Cherstvy, and E. Barkai, Anomalous diffusion models and their properties: Non-stationarity, non-ergodicity, and ageing at the centenary of single particle tracking, *Phys. Chem. Chem. Phys.* **16**, 24128 (2014).
- [35] G. M. Viswanathan, V. Afanasyev, S. V. Buldyrev, E. J. Murphy, P. A. Prince, and H. E. Stanley, Lévy flight search patterns of wandering albatrosses, *Nature* **381**, 413–415 (1996).
- [36] G. M. Viswanathan, S. V. Buldyrev, S. Havlin, M. G. da Luz, E. P. Raposo, and H. E. Stanley, Optimizing the success of random searches, *Nature* **401**, 911–914 (1999).
- [37] G. M. Viswanathan, M. G. E. da Luz, E. P. Raposo, and H. E. Stanley, *The Physics of Foraging: An Introduction to Random Searches and Biological Encounters* (Cambridge University Press, 2011).
- [38] M. A. Lomholt, T. Ambjörnsson, and R. Metzler, Optimal target search on a fast-folding polymer chain with volume exchange, *Phys. Rev. Lett.* **95**, 260603 (2005).
- [39] M. A. Lomholt, K. Tal, R. Metzler, and K. Joseph, Lévy strategies in intermittent search processes are advantageous, *Proc. Natl. Acad. Sci.* **105**, 11055 (2008).
- [40] V. V. Palyulin, G. Blackburn, M. A. Lomholt, N. W. Watkins, R. Metzler, R. Klages, and A. V. Chechkin, First passage and first hitting times of Lévy flights and Lévy walks, *New J. Phys.* **21**, 103028 (2019).
- [41] D. Boyer, G. Ramos-Fernández, O. Miramontes, J. L. Mateos, G. Cocho, H. Larralde, H. Ramos, and F. Rojas, Scale-free foraging by primates emerges from their interaction with a complex environment, *Proc. R. Soc. B* **273**, 1743 (2006).
- [42] M. S. Song, H. C. Moon, J.-H. Jeon, and H. Y. Park, Neuronal messenger ribonucleoprotein transport follows an aging Lévy walk, *Nat. Comm.* **9**, 344 (2018).
- [43] A. V. Weigel, B. Simon, M. M. Tamkun, and D. Krapf, Ergodic and nonergodic processes coexist in the plasma membrane as observed by single-molecule tracking, *Proc. Natl. Acad. Sci.* **108**, 6438 (2011).
- [44] D. Freedman and P. Diaconis, On the histogram as a density estimator: L2 theory, *Z. Wahrsch. Verw. Geb.* **57**, 453–476 (1981).
- [45] A. Clauset, C. R. Shalizi, and M. E. Newman, Power-law distributions in empirical data, *SIAM Rev.* **51**, 661–703 (2009).
- [46] D. Langlois, D. Cousineau, and J. P. Thivierge, Maximum likelihood estimators for truncated and censored power-law distributions show how neuronal avalanches may be misevaluated, *Phys. Rev. E* **89**, 012709 (2014).
- [47] M. Vahabi, J. H. P. Schulz, B. Shokri, and R. Metzler, Area coverage of radial Lévy flights with periodic boundary conditions, *Phys. Rev. E* **87**, 042136 (2013).
- [48] D. Froemberg and E. Barkai, Random time averaged diffusivities for Lévy walks, *Eur. Phys. J. B* **86**, 331 (2013).

ACKNOWLEDGMENTS

We thank Erik Kalz and Andrey G. Cherstvy for helpful discussions. We acknowledge the German Science Foundation (DFG, Grant ME 1535/22-1 and CRC Data assimilation, Grant 318763901, project B10) for support.